Historical Analysis of Champion Photovoltaic Module Efficiencies

Sarah Kurtz[1], Ingrid Repins[1], Wyatt K. Metzger[1], Pierre J. Verlinden[2], Susan Huang[3], Stuart Bowden[4], Ian Tappan[1], Keith Emery[1], Larry Kazmerski[1], Dean Levi[1]

[1]National Renewable Energy Laboratory, Golden, CO, USA
[2]State Key Laboratory of PV Science and Technology, Trina Solar, ChangZhou, 213031 China
[3]ManTech International, Herndon, VA, USA
[4]Arizona State University, Tempe, AZ, USA

***Abstract* — Champion PV cell and module efficiencies have been reported in Progress in PV since 1993. Following the evolution of these efficiencies enables researchers to track the progress of various technologies. NREL has maintained an historical chart of the champion cell efficiencies, but has not published a similar chart of champion module efficiencies. Here, we analyze champion module efficiencies and compare them to champion cell efficiencies to better understand technology trends over the last three decades, highlighting that, in some cases, module efficiencies exceed 90% of cell efficiencies. Recommendations are provided on how to change the data collection and reporting for champion efficiencies to increase the value of these records.**

I. Introduction

The conversion efficiency of light to electricity is one of the most important attributes of a photovoltaic (PV) technology. The National Renewable Energy Laboratory (NREL) has been maintaining a chart of the best research-cell efficiencies as a function of time, independent of cell size and the type of area measurement (aperture, designated, or total) [1]. As the PV industry matures, it is also useful to track total-area module efficiencies, both for champion and production devices. Over the years, many papers have tracked the progress of solar cell and module efficiencies [2-6]. Following these data is complicated by the changing methods of characterizing efficiencies as well as the many different types of cell and module design.

During the development of PV devices, focusing on the improvement of cell structures is important. However, in the ultimate deployment of PV in the field, these cell structures need to be incorporated into a module, which requires development of interconnects, packaging, by-pass diodes and, sometimes, power electronics. Integrating a cell into a module results in improvements in some areas, such as light trapping (reflected light by the ribbons, busbars and fingers can be internally reflected back toward the cell surface) and stability in the field, and power losses in others, such as losses due to series resistance and light being reflected by the front surface of the glass and by the backsheet between cells. Studying the performance of PV at the module level may also guide research towards defining the final form of the device. For example, developing novel light management designs that are optimized for the entire package including encapsulant, glass frontsheet, backsheet, light-trapping features (light capturing ribbon or LCR, light reflective film or LRF), and the anti-reflection coating (ARC) on the glass. It is useful to consider not only champion efficiencies, but also average production efficiencies as a function of time. For example, production module efficiencies have been summarized based on advertised efficiencies from websites [7,8].

For modules constructed from individual cells, the total module power divided by the sum of the cell power, called Cell-to-Module (CTM) ratio, can be considered as an important parameter to optimize the module design, but this method can be misleading. For example, this CTM ratio can be increased by just increasing the gap between cells, which results in increasing the power output but decreases the module efficiency and increases the levelized cost of electricity (LCOE). Metrics characterizing the relative performance of modules and cells vary; here, we consider for each technology the ratio of the champion module efficiency to the champion cell efficiency at a given time.

Historically, the Progress in Photovoltaics (PIP) charts have reported efficiencies using aperture area, designated area, or total area [3]. For measurements of cell efficiencies, measurements other than total area may be more useful. For example, a concentrator cell that is illuminated through concentrating optics may have light incident on only a part of the cell. It is useful to understand the conversion efficiency for that area rather than the efficiency for the larger area, including area that is not illuminated. Also, for some cells and mini-modules, measurement of the total area efficiency may be challenging and use of an aperture can reduce the uncertainty of the measurement. However, measurements of commercial module efficiencies are most useful when reported relative to the *total* area because the total-area efficiency captures edge effects and represent the performance of the product in the field. While not always available, the most useful metric for modules is the efficiency relative to the *total* area of the module.

This paper summarizes the historical champion module and cell efficiency data for each technology, including Si, CdTe, CIGS, amorphous silicon, organic, perovskite and III-V technologies and undertakes to define a "Best module efficiency chart". The time evolution of the champion efficiencies is discussed and the cell and module efficiency ratios are compared. Recommendations are made about how maintaining a "Best module efficiency chart" and related data can be most useful to the community in the future.

Pursuant to the DOE Public Access Plan, this document represents the authors' peer-reviewed, accepted manuscript. The published version of the article is available from the relevant publisher.

II. Data Collection Methods

The existing "Best Research-cell Efficiencies" chart [1] includes efficiencies reported in the Progress in PV (PIP) Efficiency Tables [3] as well as efficiencies that were measured at NREL, but were not selected for publication in the PIP tables. For this study, cell and module efficiencies were taken from the PIP Efficiency Tables and additional data were included from NREL's historical "Best Research-cell Efficiencies" chart as well as other data that would meet the PIP Table's quality requirements, but did not meet PIP Table's definition of a new record (see discussion in Section IV.B).

For simplicity, we have omitted some technologies with limited data, such as very-thin (e.g. 2-µm-thick) silicon, dye-sensitized cells, and non-III-V technologies measured under light concentration.

III. Data Summaries

A. All-technology module efficiency summary

A summary of reported module efficiencies for all technologies is shown in Fig. 1. Comparison of these efficiencies is complicated by the strong dependence of achievable efficiency on the module size. This graph provides a counterpart to the "Best Research-cell Efficiencies" chart that NREL has published [1], but scales the size of the point to the area of the module to emphasize the larger modules, while allowing visualization of all data. Modules with areas greater than 200 cm^2 are included.

As expected, the multijunction III-V data demonstrate the highest efficiencies (especially for the concentrator modules). The mono-crystalline silicon data are next highest. Champion CdTe and CIGS module efficiencies are now approaching the multi-crystalline silicon efficiencies. The data are explored in more detail by technology in the following sections; discussion and recommendations for continued tracking of module efficiencies are summarized in the final section.

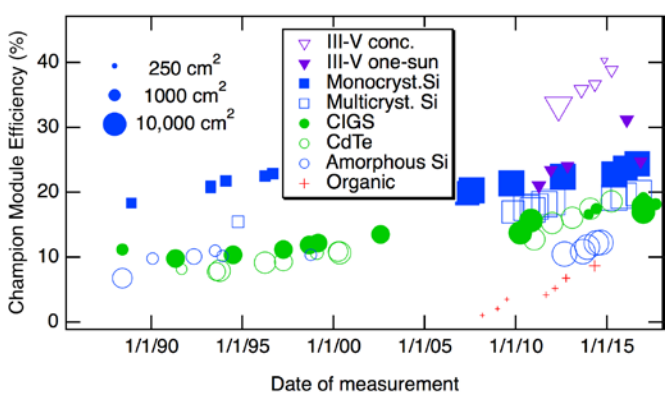

Fig. 1. Champion module efficiencies by technology. The symbols differentiate modules by technology, as indicated in the legend. The symbol size reflects the module area, as indicated.

B. Silicon

A summary of reported silicon cell and module efficiencies is shown in Fig. 2. The legend uses the abbreviations "AlBSF" for a conventional planar back-contact cell (including the metal-wrap-through approach and a variety of other early designs), "PassC" for passivated-contact (also referred to as carrier-selective contacts) solar cells (including heterojunction with intrinsic thin (HIT) layer [9] and the TOPCon [10] technology), "IBC" for interdigitated back contact [11], and "PERC" for passivated emitter; rear contact or rear locally diffused (PERL) technology [5,12]. Some of the many variations on these that are not differentiated in this legend include use of ion implantation, type of surface texturing, type of passivation, absorber thickness and/or type of wafer, and buried laser-groove contacts. The categorization of some structures may be debated. For example, the latest cells combining an IBC structure with passivated contacts using amorphous-silicon developed by Kaneka, Panasonic and Sharp are plotted twice, as both PassC and IBC. We found that these four categories helped to differentiate the timelines of development of the various structures, and suggest that this or a similar categorization may be useful in tracking development of silicon cells in the future, as discussed below.

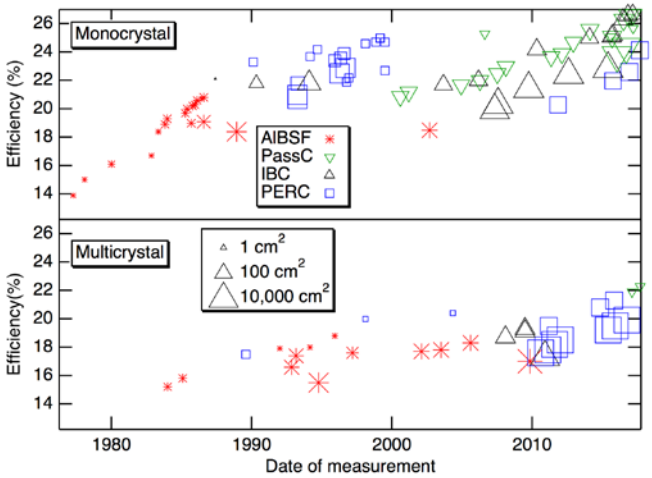

Fig. 2. Champion efficiencies for silicon cells and modules as a function of time, type and area. The symbol size reflects the device area, as indicated. Data for monocrystalline and multicrystalline devices are shown in the top and lower panels, respectively, with both panels using the same symbol designations.

Fig. 2 shows how monocrystalline devices have consistently outperformed multicrystalline devices, but shows also that the gap between the best efficiencies of mono- and multi-crystalline devices of the same area and the same type has stayed relatively constant for the highest values. Although the "Best Research-cell Efficiency" chart from NREL implies that there was no improvement in efficiency of monocrystalline silicon cells between 1999 (25% "designated area" efficiency for a 4 cm^2 PERL cell) and 2014, Fig. 2 clearly shows that there has been a continuous improvement in efficiency for large devices, even surpassing the 1999 small-area cell record.

Pursuant to the DOE Public Access Plan, this document represents the authors' peer-reviewed, accepted manuscript. The published version of the article is available from the relevant publisher.

It also shows how the types of cells and modules reporting the highest efficiencies have evolved with time. The early increase in efficiency of the conventional cells made with aluminum back-surface fields were quickly surpassed by the higher efficiencies of the PERC and PERL cells made at the University of New South Wales (UNSW). Between about 1985 and 2000, in parallel with development of the PERL cells, IBC cells were developed at Stanford University and commercialized at SunPower, though the early commercial deployment was mostly for concentrator, solar race car and solar airplane applications. Development of the HIT cells and associated commercial modules at Sanyo (in the passivated-contact category) came a little later.

The delay between achieving a high small-cell efficiency and a high large-cell efficiency appears to be highly variable, based on the data in Fig. 2. More careful analysis of the data suggests that the time for module implementation depends largely on whether the champion cells are being reported by an R&D lab or by a company developing the cells for commercial implementation. Typically, the need to identify low-cost manufacturing processes for the more complex processing sequences associated with the PERC and IBC approaches was a limiting step. For example, SunPower/Honda reported in 1993 an efficiency of 21.6% for a small IBC module (862 cm^2) [13]. The IBC cells, designed for a Honda solar race car [14], were relatively small (17.6 cm^2) and were fabricated with an expensive process using photolithography, vacuum-evaporated ARC and sputtered metallization. It took about another 10 years for SunPower to establish a low-cost IBC process and to commercialize a full-size PV module with large-area (125 x 125 mm^2) cells of similar efficiency. Another example is the development of high-efficiency multi-crystalline cells. In 2004 Fraunhofer Institute ISE reported a 20.4% multicrystalline silicon solar cell [15]. The cell was only 1 cm^2 in size. It took another 10 years for the PV industry to report an equivalent efficiency on full-size cells. In 2014, Trina Solar reported a 20.8% efficient multi-crystalline solar cell of 243 cm^2 [16], a result that was upgraded to 21.25% just one year later [17]. UNSW reported an efficiency of 22.7% (later revised to 22.9%) for a small (778 cm^2) mono-Si PERC module in 1996 [18]. A number of companies today have developed full-size PERC modules, but these champion efficiencies have not been tracked in the PIP Efficiency Tables because they have lower efficiencies than the PassC or IBC modules. For example, Trina Solar reported a 22.6%-efficient PERC monocrystalline cell in December 2016 [19,20], which is less than the 25%-26% efficiencies reported for IBC and PassC cells in the same time period. While this could be interpreted to imply that the PERC cells are inferior in terms of efficiency, there is substantial commercial interest in PERC modules in terms of cost effectiveness; tracking the evolution of efficiencies for large cells and modules aids in assessing this commercial interest. This shows how important it is to present efficiency records from the perspective of the type of solar cell structure and solar cell or module size. For careful analyses, it is also essential to track the type of area (total area vs. dedicated or aperture area) used to measure the efficiency.

Historically, efficiencies for multicrystalline devices have been ~4% (absolute) lower in efficiency than monocrystalline cells or modules of similar size. However, recently, the difference in mono- versus multi-crystalline Si efficiency champions has narrowed to < 2% for PERC cells, mainly due to the recent development of high-performance multicrystalline substrates with smaller grain size and lower dislocation density. As seen in Fig. 2, champion multi-crystalline silicon efficiencies today are mostly dominated by PERC approaches, while the IBC and PassC designs typically have higher efficiencies for monocrystalline silicon, reflecting the ~4% difference between mono- and multi-crystalline cells for the IBC and PassC designs, but the smaller difference for the PERC designs. This difference may reflect the inability of the multi-crystalline devices in replicating the high open-circuit voltages (V_{oc}) achieved for the IBC and PassC mono-crystalline cells, while the V_{oc}s for the mono- and multi-crystalline Si PERC cells are closer.

C. Thin-film - CdTe

CdTe cell (open circles) and module efficiencies are shown in Fig. 3. Throughout the 1980s CdTe was deposited by various techniques including spray deposition, electrodeposition, screen printing, physical vapor deposition, molecular organic chemical vapor deposition, and atomic layer epitaxy [21]. Record cell efficiencies were around 11%. Cell efficiency improved significantly to 15.8% in the early 1990s when the University of Southern Florida deposited CdTe by close-spaced sublimation onto glass/SnO_2:F/SnO_2/CdS substrates at ~600°C. This film stack was subsequently annealed in $CdCl_2$, and then a back contact process that diffused Cu into the CdTe was applied [22,23]. NREL increased cell efficiency to 16.7% in the early 2000s by replacing the SnO_2 bilayer with Cd_2SnO_4 and $ZnSnO_4$ and sputtering nanocrystalline CdS:O to reach J_{sc} > 26 mA/cm^2 [24]. This record stood for about a decade because it was difficult to introduce further improvements in the

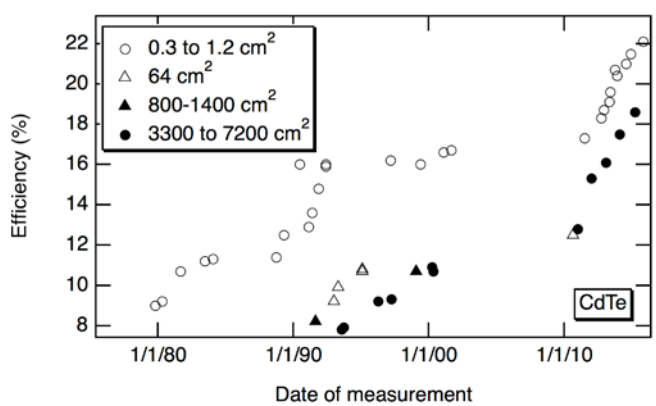

Fig. 3. Champion efficiencies for CdTe devices.

Pursuant to the DOE Public Access Plan, this document represents the authors' peer-reviewed, accepted manuscript. The published version of the article is available from the relevant publisher.

CdTe defect chemistry and film stack. In addition, research focus shifted to understanding and translating research cell efficiency to industry.

The large gap between module efficiencies and cell efficiencies from the 1990s to 2010 was partly because industry during this time was not able to replicate record cell efficiencies internally or across large areas in production. Another cause for the large gap is that CdTe module-to-cell efficiency ratios are ~ 85-90% when optimized. Monolithic modules are typically made with hundreds of cells. The scribes for interconnecting these cells, edge delete, and other module features contribute to areas that do not convert sunlight into electricity. Large modules also have series resistance from the transparent conducting oxide that record cells can avoid with specialized cell structures and contact schemes.

The gap between cell and module efficiencies narrowed after 2011 to optimum values. More aggressive efficiency improvements were driven in part because the $/$W_p$ cost of multi-Si panels began to compete with CdTe panels directly, so CdTe panels needed to improve and match multi-Si performance directly. First Solar and PrimeStar Solar/General Electric traded world record cell efficiencies, and at the same time produced uniform modules with similar aperture efficiency to champion cells. In 2013, the companies merged their technologies and continued to increase performance. The thickness of the absorptive CdS window layer was progressively decreased and eventually replaced with CdSeTe grading. Along with other optical improvements, this increased the photocurrent from ~26 to more than 31 mA/cm^2 [25,26]. Back contact improvements increased stability and fill factor. At the same time, carrier lifetimes steadily improved partly from better interface quality and the introduction of CdSeTe [27,28]. As a result of these improvements, CdTe modules have achieved similar performance to multi-Si and costs competitive with fossil fuels in many locations [29].

For decades, CdTe hole density has been limited to the order of 10^{14} cm^{-3}. Recent work indicates p-CdTe can simultaneously achieve hole densities exceeding 10^{16} cm^{-3} and lifetimes greater than 100 ns [30]. So there is more opportunity to significantly increase CdTe cell and module efficiencies [31]. In addition, there is still a gap between record modules and production modules that will decrease as new technology is transferred into production.

Historically, commercial CdTe modules have been somewhat smaller than silicon modules, somewhat increasing balance of system costs because of the need to handle a greater number of modules. To address this, First Solar is preparing to launch their Series 6 modules, which will be 120 cm X 180 cm (~21,000 cm^2) and about 400 W, thereby competing directly with the power rating of even the largest silicon modules.

D. Thin-film - CIGS

A summary of CIGS cell, submodule, and module efficiencies is shown in Fig. 4. The history of CIGS cell efficiencies shows four periods: 1) steady efficiency increase with empirical optimization of the absorber and heterojunction partners up to 1995 [32]; 2) rapid efficiency increase with the introduction of Ga and the associated bandgap grading from 1995 to 1999 [33,34]; 3) modest efficiency increases from 2000 to 2010 as tighter process control and finer understanding of multiple layers in the devices were developed [35,36]; and 4) a period of more rapid increases from 2010 to the present, reflecting both larger-scale industrial involvement in record-setting devices [37] and the introduction of alkali surface treatments [38]. CIGS cell efficiencies reached 18-20% in the 1995-2000 timeframe, while CdTe cell efficiencies reached this range only after 2010. At present, record cell efficiencies are similar for CIGS (22.6% for 0.4 cm^2), CdTe (22.1% for 0.5 cm^2), multi-crystalline Si (21.9% [1] for 4 cm^2), and perovskites (22.1% for 0.1 cm^2) [39].

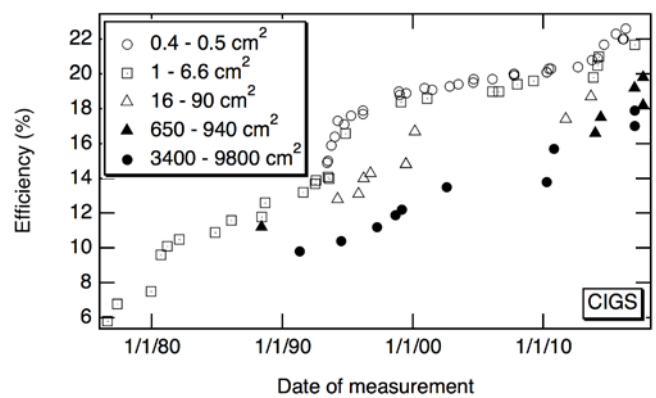

Fig. 4. Champion efficiencies for CIGS devices.

CIGS module efficiencies have increased steadily over the years, largely mirroring the size of the industrial effort. The difference between small cell and module efficiency ($\Delta\eta$) was also decreased. Such decreases can be associated with maturation of industrial process control, implementation of research advances on the manufacturing line, and optimization of module-specific features such as scribe lines or grids on singulated cells [40].

Fabrication of champion cells and modules are not tied to a particular CIGS absorber deposition technique. Champion cells have been made by co-evaporation [33] and sequential-sputtering with selenization [37]. Champion modules have been made by sequential sputtering with selenization [37] at Solar Frontier, co-sputtering [41] at Miasole, and co-evaporation [33] at Solibro.

The difference between cell and module efficiencies for CIGS has tended to be even greater than for CdTe, although there are very few cases where a champion cell was reported

[1] Fraunhofer ISE announced a 22.3% efficiency for a 4 cm^2 cell in September 2017.

Pursuant to the DOE Public Access Plan, this document represents the authors' peer-reviewed, accepted manuscript. The published version of the article is available from the relevant publisher.

for the same material used in the module. Recently, small CIGS modules have achieved efficiencies > 80% of the cell efficiency, but, commonly, champion efficiencies for CIGS modules have been closer to 70% of the champion cell efficiencies, implying substantial opportunity for improvement. Experimental and modeling studies on CIGS suggest that $\Delta\eta$ can ultimately be reduced to 1-2% [42,43], which is similar to the 90-95% cell-to-module efficiency ratio noted for Si.

E. Thin-film - Other

A summary of amorphous silicon cell and module efficiencies is shown in Fig. 5. Similar to CdTe and CIGS, in the decade between 2000 and 2010, more effort was placed on increasing manufacturing, resulting in less increase in cell efficiency. Commercial interest in amorphous silicon has been challenged by the higher efficiencies of CIGS and CdTe modules. Nevertheless, very large amorphous silicon modules (area > 14,000 cm^2) were demonstrated with stabilized efficiency > 12% in recent years [44]. The champion efficiencies of large-area amorphous silicon modules began to approach 90% of champion cell efficiencies of that time, though a direct comparison between cells and module made on the same hardware was not found.

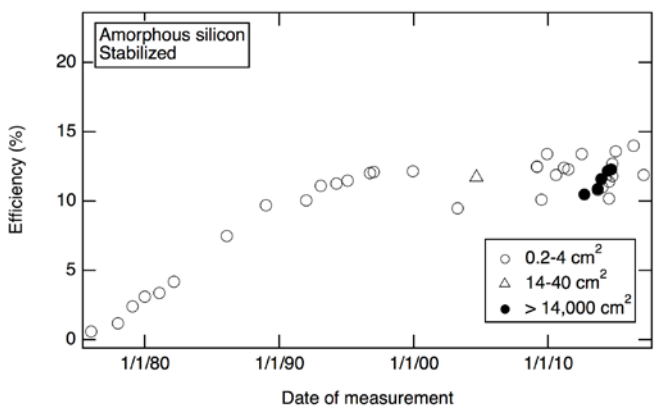

Fig. 5. Champion efficiencies for amorphous silicon devices.

A summary of organic (OPV) cell and module efficiencies is shown in Fig. 6. A champion OPV cell efficiency reached 12.1% for a 0.04 cm^2 cell in 2017 [39], while a small-area (802 cm^2) module efficiency was reported to reach just 8.7% [45]. Recent efficiencies for perovskite cells are also shown in Fig. 6. Perovskite device efficiencies have increased rapidly, leveraging knowledge gained with organic cells. The perovskites have been difficult to scale to large area, but progress is being made as evidenced by the most recent data point in Fig. 6, which is the unstabilized efficiency for a 36 cm^2 minimodule [46].

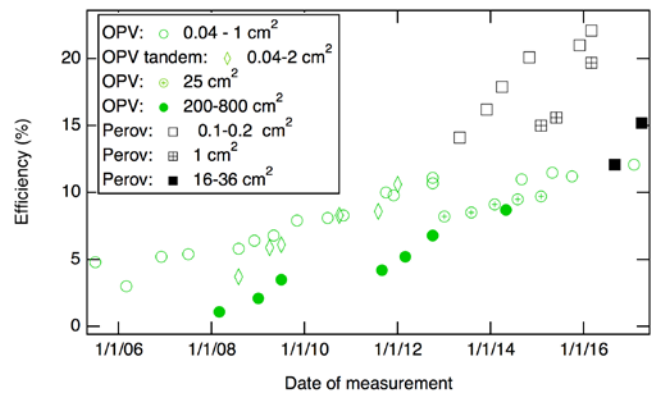

Fig. 6. Champion efficiencies for organic and perovskite devices.

F. III-V

A summary of one-sun III-V cell and small-module efficiencies is shown in Fig. 7. Commercial development of III-V cells using chemical-vapor deposition (also known as organometallic, vapor phase epitaxy, OMVPE) was originally focused on space applications, but after the year 2000, interest in concentrator cells for terrestrial applications increased, eventually resulting in small concentrator modules with efficiencies approaching 40%, as shown in Fig. 8 [47].

In the late 1980s, after the two-junction GaInP/GaAs cell demonstrated higher efficiencies than single-junction GaAs cells, the space community rapidly moved toward multijunction technology, including both the GaInP/GaAs two-junction cells grown on germanium substrates (because of germanium's lower cost, but similar lattice constant compared with GaAs) and similar three-junction cells that incorporated an active germanium junction. Efficiencies of both one-sun and concentrator cells increased steadily after the year 2000, with champion concentrator cell efficiencies increasing ~1%/year, on average, between 2000 and 2014.

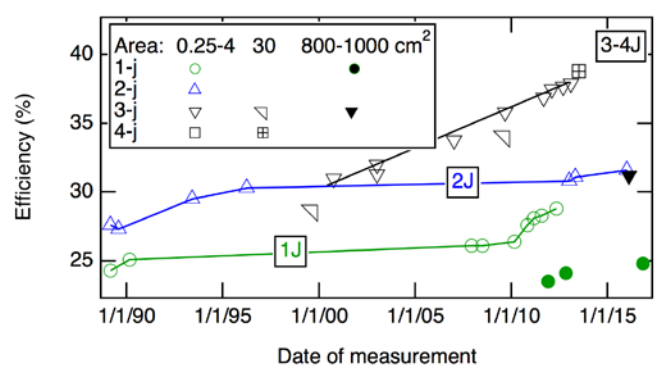

Fig. 7. Champion efficiencies for one-sun III-V devices. Lines are added to guide the eye: green for 1-junction cells, blue for 2-junction cells and black for 3- and 4-junction cells.

Pursuant to the DOE Public Access Plan, this document represents the authors' peer-reviewed, accepted manuscript. The published version of the article is available from the relevant publisher.

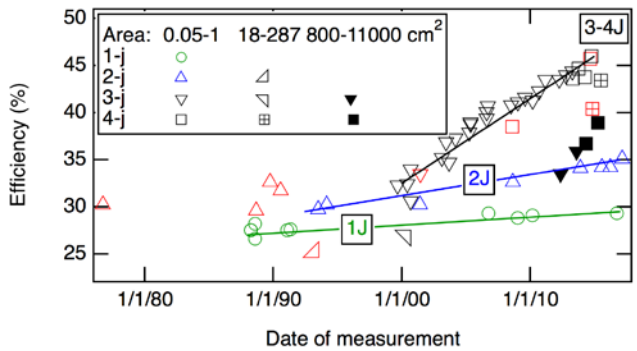

Fig. 8. Champion efficiencies for concentrator III-V devices. These efficiencies are measured using the AM1.5 Direct spectrum. Lines are added to guide the eye: green for 1-junction cells, blue for 2-junction cells and black for 3- and 4-junction cells. The red symbols indicate 3- or 4-terminal measurements for mechanical stacks or spectrum-split configurations.

The germanium junction of the GaInP/GaAs/Ge cell was capable of generating almost twice the photocurrent of the GaInP and GaAs junctions, implying that addition of a 1-eV third junction [48] could increase the efficiency of a three-junction cell (by increasing the photovoltage with a similar photocurrent) or turn the three-junction GaInP/GaAs/Ge cell into a four-junction GaInP/GaAs/1-eV/Ge cell. Several strategies for assembling the multiple junctions were pursued in parallel including use of lattice-mismatched alloys [49,50], dilute-nitride alloys [51], and wafer bonding [52], mechanical stacking [53], or spectrum splitting [54].

One approach to the 1-eV material was to allow the lattice constant to vary. For example, addition of indium to GaAs increases the lattice constant while decreasing the band gap [49]. The inverted-metamorphic (IMM) approach deposited first the lattice-matched GaInP and GaAs in an inverted configuration, then deposited a metamorphic layer to grade to the lattice constant of the 1-eV GaInAs [50]. The structure was inverted and the substrate removed during processing. The IMM approach was reported to have set its first record efficiency in 2006 with a 40%-efficient GaInP/GaAs/GaInAs cell at 143 suns concentration [55].

The dilute-nitride approach was pursued when it was found that the addition of a small amount of nitrogen to GaAs reduced its band gap significantly, enabling a lattice-matched, 1-eV material to be grown on germanium before growth of the lattice-matched top cells. However, despite the apparent simplicity of this approach, the dilute nitride materials grown by OMVPE showed disappointing quality and progress was slow for many years [56]. Then, Solar Junction demonstrated that molecular beam epitaxy could grow GaInAsN with higher optoelectronic quality and in 2011 set a record of 43.5% with a three-junction cell using a dilute nitride as the third junction [51].

Additionally, a large variety of combinations of materials have been brought together in mechanical stacks, using wafer bonding, or by spectrum splitting. The current world record is a 46%-efficient, 4-junction concentrator cell with a GaInP/GaAs cell wafer bonded by Soitec to a GaInAsP/GaInAs cell [52]. Including additional junctions has resulted in high efficiencies, but the full benefit of a 5- or 6-junction cell has not yet been realized.

While the bulk of III-V solar cell R&D has focused on adding more junctions, between 2010 and 2012 Alta Devices demonstrated how enhanced optical design of a single-junction GaAs cell to improve photon recycling can lead to higher photovoltages [57]. They increased the champion GaAs cell efficiency to 28.8% [58] in a short time. Alta Devices is one of the few companies exploring lower-cost approaches to depositing III-V materials with the goal of addressing one-sun terrestrial applications in a cost-effective manner and, in 2016, made a 24.8% efficient single-junction GaAs module with 865 cm^2 area [39]. Sharp made a three-junction 968 cm^2 module with 31.2% efficiency in the same year [59].

While III-V cell and module efficiencies are quite attractive, the industry is working to reduce cost, especially to keep up with the rapid cost reduction of silicon modules.

Only one III-V module > 10,000 cm^2 is reported in the efficiency tables, with an efficiency of 33.5%, about 75% of the efficiency of champion cells at that time [60].

IV. Discussion and Conclusions

A. Comparison of Cell and Module Efficiencies

As discussed above, module efficiencies approach, but do not quite reach, the corresponding cell efficiencies. The dependence of efficiency on size of cell or module coupled with the differences between using aperture, designated, or total area efficiencies introduces a few per cent uncertainty in defining how to characterize the cell and module efficiencies as a function of time. This complicates the comparison between cell and module efficiencies because the effects of size and area definition may approach the difference between the cell and module efficiencies in some cases. Also, the comparison for silicon modules, for which a company can hand pick a set of champion cells to assemble into a single module, is fundamentally different from the comparison for thin-film modules. For silicon, the comparison today may be between a large-area (100-250 cm^2) cell and a full-size (12,000-16,000 cm^2) module, while comparisons of older data are likely to be for smaller cells and smaller modules. Similarly, comparisons for thin-film products are often for cells < 1 cm^2 and for smaller modules that are < 10,000 cm^2. Careful review of Figs. 1-8 shows that higher efficiencies tend to be reported for smaller devices for all technologies, though this does not necessarily hold universally.

Despite that the comparisons may not be equivalent between technologies or even from year to year, it is interesting to consider the difference between champion cell and module efficiencies, using the available data regardless of the size of the

Pursuant to the DOE Public Access Plan, this document represents the authors' peer-reviewed, accepted manuscript. The published version of the article is available from the relevant publisher.

cells and modules. The ratio of champion module efficiency to champion cell efficiency is shown in Fig. 9 as a function of cumulative deployment volume for each of the primary technologies. The lines were derived using the champion cell and module efficiencies reported at the end of each year. Often, these efficiencies were reported by different organizations, sometimes with different types of cells. In a handful of cases, champion cell and module efficiencies were identified from the same organization within a few months, facilitating a direct comparison of module efficiencies with the efficiencies of the cells that were (presumably) used to make those modules. In these cases, points are plotted alongside of the lines in Fig. 9.

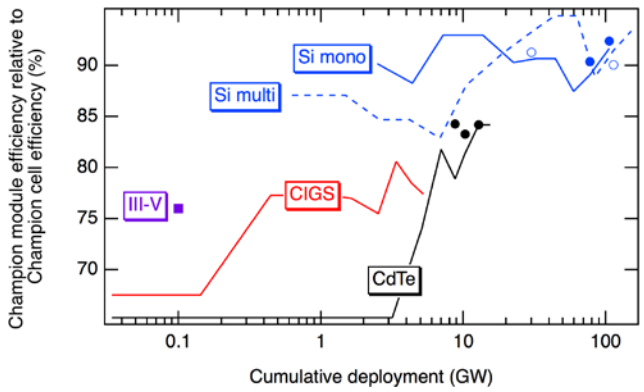

Fig. 9. Ratio of champion module efficiency to champion cell efficiency as a function of cumulative deployment by technology. The lines reflect annual data; the points reflect comparisons of cell and module efficiencies from a single organization, as discussed in the text. The solid (open) blue circles are for mono (multi) crystalline silicon.

As shown in Fig. 9, currently, the module-to-cell efficiency ratios for crystalline silicon are ~ 90% or slightly higher, a tremendous achievement for the community. The ratios for CdTe are falling around 84% and the data for CIGS have been increasing past 80%. The 76% data point for a multijunction III-V module shown in Fig. 9 is estimated for a large concentrator module. A small (865 cm^2) one-sun GaAs module achieved ~86% of the corresponding cell efficiency, but is not shown on the graph because of the low deployment volume. None of these module efficiencies was reported for the total area of the module (most were measured using an aperture area). From the earlier figures, it's clear that both cell and module efficiencies are continuing to improve for all technologies. It's less clear whether the module-to-cell efficiency ratio will improve for all technologies.

B. Recommendations for champion module efficiency chart

A comparison of module efficiencies for all of the technologies is shown in Fig. 1, omitting data for modules < 200 cm^2. The choice of the size range to include is challenging; the size of a commercial module today varies by technology and many champion efficiencies are reported for smaller modules. Even if a module is of a commercial size, champion specimens are not always taken from the production line, but fabricated to define what can be achieved, and record efficiencies are usually measured behind an aperture smaller than the physical module. Inclusion of "demonstration" and small modules allows us to track the technology development in a way that mirrors the Research-Cell Efficiencies Chart, providing value despite the lack of equivalence to commercial products. In Fig. 1, we chose to include modules > 200 cm^2 in order to better track the OPV development in the 2008-2009 timeframe, but we suggest that a requirement of > 300 cm^2 would be preferable by requiring a "module" to be bigger than the largest silicon cells. On the other hand, even the 200-cm^2 choice does not enable us to find a perovskite module to include in the chart at this time.

In this paper, we have highlighted the value of tracking different types of silicon cells, but we have not attempted to differentiate these in Fig. 1 because of the complexity of the resulting graph. Nevertheless, there is no reason not to record information about the type of technology and to record efficiencies even when it may not be the highest efficiency in the more general technology category. The tracking of efficiencies for different types of structures may be more important for modules than for cells because commercial module development is largely driven by which structures can be made with an inexpensive manufacturing process. If an expensive process is used to set an efficiency record and less-expensive processes are required to pass that record before a new record is recorded, we lose our ability to track progress for some of the most important commercial technologies.

As discussed above, the utility of the module efficiency could be increased by requiring total-area measurements. Currently, the PIP tables report most module efficiencies based on an aperture-area measurement, while it could be quite straightforward to report total-area efficiencies, which are the values that are meaningful to the customer to calculate LCOE.

Based on the discussions above, for documenting module efficiencies, we recommend:

- Creating and updating a graph similar to that in Fig. 1 to complement the existing "Best Research-Cell Efficiency" graph using module efficiency data measured at recognized calibration laboratories under standard test conditions to ensure data quality. The graph should differentiate technology type by symbol and area of each module by the size of the symbol. The data used to create the graph should be available for download as a sortable spreadsheet.
- Defining a module (which we assume to have more than one cell) to be > 300 cm^2 for inclusion in the graph, while including data in the accompanying spreadsheet for small mini-modules for easy reference.
- Recording module efficiencies if they represent an advance in efficiency for a specific size module. It should not be a requirement to surpass the efficiency of a smaller module to be

Pursuant to the DOE Public Access Plan, this document represents the authors' peer-reviewed, accepted manuscript. The published version of the article is available from the relevant publisher.

included since we would like to be able to track progress for large modules as well as small modules and both history and logic suggest that small-area modules will dominate the reported efficiencies if size is not considered.

• Including a total-area efficiency if it surpasses other total-area efficiencies even if it does not surpass the record aperture-area or designated-area efficiency for that size module.

• Creating a third graph summarizing only total-area module efficiencies as data for total-area module efficiencies become more available.

• Recording high efficiencies for a larger number of technology categories, such as the additional categories used in Fig. 2. These may or may not be differentiated in the Fig. 1-type summary graph, but could be differentiated in the corresponding spreadsheet.

Additionally, we recommend keeping the Best Module Efficiencies Chart consistent with the Best Research-Cell Efficiencies Chart by:

• Placing similar requirements on recorded cell efficiencies as recommended for module efficiencies including measurements done at recognized calibration laboratories, tracking a larger number of technology categories, and maintaining a spreadsheet of data that includes more information than in the summary graph.

• Recording the type of area measurement in the summary spreadsheet to encourage consideration of how this affects the results.

• Recording, as recommended for modules, total-area cell efficiencies, when relevant, even when these are lower efficiencies than shown in the historical records for smaller cells or for cells measured with designated or aperture areas.

C. Conclusions

Champion cell and module efficiencies for all photovoltaic technologies have continued to increase in recent years, with the ratio of the reported champion module efficiency to champion cell efficiency frequently exceeding 90% for crystalline silicon technologies, reaching 90% for CdTe and exceeding 80% for CIGS. The time for implementation of a new type of cell into a similar module has been highly variable, sometimes requiring 10-20 years, often reflecting the time needed to develop a low-cost manufacturing process for a given cell design.

The tracking of champion efficiencies has often excluded data for the most commercially relevant devices because of the naturally higher efficiencies that can be expected for smaller devices and for more expensive fabrication processes. Recommendations were given on how to track champion module efficiencies to best support analysis of industry progress especially with regard to recording efficiencies for large and commercially relevant modules using total-area measurements.

Acknowledgements

This work was supported by the U.S. Department of Energy under Contract No. DE-AC36-08GO28308 with the National Renewable Energy Laboratory. Funding provided by U.S. Department of Energy Office of Energy Efficiency and Renewable Energy Solar Energy Technologies Office.

References

[1] https://www.nrel.gov/pv/assets/images/efficiency-chart.png, accessed 2017.

[2] H. Watanabe, "Improvements in multicrystalline silicon solar cells," in *Proceedings of 6th International Photovoltaic Science and Engineering*, 1989, p. 162.

[3] M.A. Green, and K. Emery, "Solar cell efficiency tables," *Progress in Photovoltaics: Research and Applications*, vol. 1, pp. 25-29, http://dx.doi.org/10.1002/pip.4670010104, 1993.

[4] A. Goetzberger, J. Luther, and G. Willeke, "Solar cells: past, present, future," *Solar energy materials and solar cells*, vol. 74, pp. 1-11, 2002.

[5] M.A. Green, "The path to 25% silicon solar cell efficiency: History of silicon cell evolution," *Progress in Photovoltaics: Research and Applications*, vol. 17, pp. 183-189, http://dx.doi.org/10.1002/pip.892, 2009.

[6] M. Yamaguchi, T. Takamoto, K. Araki, and N. Kojima, "Recent results for concentrator photovoltaics in Japan," *Japanese Journal of Applied Physics*, vol. 55, p. 04EA05, http://stacks.iop.org/1347-4065/55/i=4S/a=04EA05, 2016.

[7] T.M. Razykov, C.S. Ferekides, D. Morel, E. Stefanakos, H.S. Ullal, and H.M. Upadhyaya, "Solar photovoltaic electricity: Current status and future prospects," *Solar Energy*, vol. 85, pp. 1580-1608, http://www.sciencedirect.com/science/article/pii/S0038092X1000366X, 2011.

[8] Y. Chen, Z. Feng, and P. Verlinden, "Assessment of module efficiency and manufacturing cost for industrial crystalline silicon and thin film technologies," in *6th World Conference on Photovoltaic Energy Conversion*, 2014, pp. 1319-1320.

[9] M. Tanaka, M. Taguchi, T. Matsuyama, T. Sawada, S. Tsuda, S. Nakano, H. Hanafusa, and Y. Kuwano, "Development of new a-Si/c-Si heterojunction solar cells: ACJ-HIT (artificially constructed junction-heterojunction with intrinsic thin-layer)," *Japanese Journal of Applied Physics*, vol. 31, p. 3518, 1992.

Pursuant to the DOE Public Access Plan, this document represents the authors' peer-reviewed, accepted manuscript. The published version of the article is available from the relevant publisher.

[10] F. Feldmann, M. Bivour, C. Reichel, M. Hermle, and S.W. Glunz, "Passivated rear contacts for high-efficiency n-type Si solar cells providing high interface passivation quality and excellent transport characteristics," *Solar Energy Materials and Solar Cells*, vol. 120, pp. 270-274, 2014.

[11] R.M. Swanson, "Method of fabricating back surface point contact solar cells," U.S. Patent # 4927770, 1990.

[12] M.A. Green, "The Passivated Emitter and Rear Cell (PERC): From conception to mass production," *Solar Energy Materials and Solar Cells*, vol. 143, pp. 190-197, http://www.sciencedirect.com/science/article/pii/S0927024815003244, 2015.

[13] M.A. Green, and K. Emery, "Solar cell efficiency tables (version 4)," *Progress in Photovoltaics: Research and Applications*, vol. 2, pp. 231-234, http://dx.doi.org/10.1002/pip.4670020307, 1994.

[14] P.J. Verlinden, R.M. Swanson, and R.A. Crane, "7000 high-efficiency cells for a dream," *Progress in Photovoltaics: Research and Applications*, vol. 2, pp. 143-152, http://dx.doi.org/10.1002/pip.4670020209, 1994.

[15] O. Schultz, S. Glunz, J. Goldschmidt, H. Lautenschlager, A. Leimenstoll, E. Schneiderlöchner, and G. Willeke "Thermal oxidation processes for high-efficiency multicrystalline silicon solar cells," in *19th European Photovoltaic Solar Energy Conference*, 2004, pp. 604-607.

[16] P. Verlinden, W. Deng, X. Zhang, Y. Yang, J. Xu, Y. Shu, P. Quan, J. Sheng, S. Zhang, and J. Bao, "Strategy, development and mass production of high-efficiency crystalline Si PV modules," in *6th World Conference on PV Energy Conversion*, Conference, 2014, pp. 485-488.

[17] M.A. Green, K. Emery, Y. Hishikawa, W. Warta, and E.D. Dunlop, "Solar cell efficiency tables (version 47)," *Progress in Photovoltaics: Research and Applications*, vol. 24, pp. 3-11, http://dx.doi.org/10.1002/pip.2728, 2016.

[18] M.A. Green, K. Emery, K. Bücher, D.L. King, and S. Igari, "Solar Cell Efficiency Tables (Version 9)," *Progress in Photovoltaics: Research and Applications*, vol. 5, pp. 51-54, http://dx.doi.org/10.1002/(SICI)1099-159X(199701/02)5:1<51::AID-PIP154>3.0.CO;2-K, 1997.

[19] "Trina Solar Announces New Efficiency Record of 22.61% for Mono-Crystalline Silicon PERC Cell", http://www.trinasolar.com/en-glb/resources/newsroom/201612192017.

[20] W. Deng, F. Ye, R. Liu, Y. Li, H. Chen, Z. Xiong, Y. Yang, Y. Chen, Y. Wang, and P.P. Altermatt, "22.61% Efficient fully Screen Printed PERC Solar Cell," in *44th IEEE Photovoltaic Specialists' Conference*, 2017.

[21] T.L. Chu, and S.S. Chu, "Recent progress in thin-film cadmium telluride solar cells," *Progress in Photovoltaics: Research and Applications*, vol. 1, pp. 31-42, 1993.

[22] T. Chu, S.S. Chu, J. Britt, C. Ferekides, C. Wang, C. Wu, and H. Ullal, "14.6% efficient thin-film cadmium telluride heterojunction solar cells," *IEEE electron device letters*, vol. 13, pp. 303-304, 1992.

[23] J. Britt, and C. Ferekides, "Thin-film CdS/CdTe solar cell with 15.8% efficiency," *Applied Physics Letters*, vol. 62, pp. 2851-2852, 1993.

[24] X. Wu, "High-efficiency polycrystalline CdTe thin-film solar cells," *Solar Energy*, vol. 77, pp. 803-814, 2004.

[25] R. Geisthardt, M. Topic, and J.R. Sites, "Status and Potential of CdTe Solar-Cell Efficiency", *IEEE Journal of Photovoltaics*, Vol. 5, pp. 1217-1221, 2015.

[26] M.A. Green, K. Emery, Y. Hishikawa, W. Warta, and E.D. Dunlop, "Solar cell efficiency tables (version 48)," *Progress in Photovoltaics: Research and Applications*, vol. 24, pp. 905-913, http://dx.doi.org/10.1002/pip.2788, 2016.

[27] A.R. Duggal, J.J. Shiang, W.H. Huber, and A.F. Halverson, "Photovoltaic devices", U.S. Patent Application # 20140376908, 2014.

[28] M. Gloeckler, I. Sankin, and Z. Zhao, "CdTe solar cells at the threshold to 20% efficiency," *IEEE Journal of Photovoltaics*, vol. 3, pp. 1389-1393, 2013.

[29] "Levelized Cost and Levelized Avoided Cost of New Generation Resources in the Annual Energy Outlook 2017", https://www.eia.gov/outlooks/aeo/pdf/electricity_generation.pdf, accessed July 2017.

[30] J.M. Burst, J.N. Duenow, D.S. Albin, E. Colegrove, M.O. Reese, J.A. Aguiar, C.-S. Jiang, M. Patel, M.M. Al-Jassim, and D. Kuciauskas, "CdTe solar cells with open-circuit voltage breaking the 1 V barrier," *Nature Energy*, vol. 1, p. 16015, 2016.

[31] A. Kanevce, M.O. Reese, T.M. Barnes, S.A. Jensen, and W.K. Metzger, "The roles of carrier concentration and interface, bulk, and grain-boundary recombination for 25% efficient CdTe solar cells," *Journal of Applied Physics*, vol. 121, p. 214506, 2017.

[32] L. Stolt, J. Hedström, J. Kessler, M. Ruckh, K.O. Velthaus, and H.W. Schock, "ZnO/CdS/$CuInSe_2$ thin-film

Pursuant to the DOE Public Access Plan, this document represents the authors' peer-reviewed, accepted manuscript. The published version of the article is available from the relevant publisher.

solar cells with improved performance," *Applied Physics Letters*, vol. 62, pp. 597-599, 1993.

[33] A.M. Gabor, J.R. Tuttle, A. Schwartzlander, A.L. Tennant, M.A. Contreras, and R. Noufi, "Band-gap engineering in Cu(In,Ga)Se_2 thin films grown from (In,Ga)$_2$Se$_3$ precursors," in *24th IEEE Photovoltaic Specialists Conference*, 1994, pp. 83-86.

[34] T. Dullweber, O. Lundberg, J. Malmström, M. Bodegård, L. Stolt, U. Rau, H.-W. Schock, and J.H. Werner, "Back surface band gap gradings in Cu(In,Ga)Se_2 solar cells," *Thin Solid Films*, vol. 387, pp. 11-13, 2001.

[35] I. Repins, M.A. Contreras, B. Egaas, C. DeHart, J. Scharf, C.L. Perkins, B. To, and R. Noufi, "19·9%-efficient ZnO/CdS/CuInGaSe_2 solar cell with 81·2% fill factor," *Progress in Photovoltaics: Research and Applications*, vol. 16, pp. 235-239, http://dx.doi.org/10.1002/pip.822, 2008.

[36] P. Jackson, R. Würz, U. Rau, J. Mattheis, M. Kurth, T. Schlötzer, G. Bilger, and J.H. Werner, "High quality baseline for high efficiency, Cu(In_{1-x},Ga_x)Se_2 solar cells," *Progress in Photovoltaics: Research and Applications*, vol. 15, pp. 507-519, http://dx.doi.org/10.1002/pip.757, 2007.

[37] R. Kamada, T. Yagioka, S. Adachi, A. Handa, K.F. Tai, T. Kato, and H. Sugimoto "New world record Cu(In,Ga)(Se,S)$_2$ thin film solar cell efficiency beyond 22%," in *43rd IEEE Photovoltaic Specialists Conference*, 2016, pp. 1287-1291, 10.1109/PVSC.2016.7749822.

[38] A. Chirila, P. Reinhard, F. Pianezzi, P. Bloesch, A.R. Uhl, C. Fella, L. Kranz, D. Keller, C. Gretener, and H. Hagendorfer, "Potassium-induced surface modification of Cu(In,Ga)Se_2 thin films for high-efficiency solar cells," *Nature Materials*, vol. 12, p. 1107, 2013.

[39] M.A. Green, Y. Hishikawa, W. Warta, E.D. Dunlop, D.H. Levi, J. Hohl-Ebinger, and A.W. Ho-Baillie, "Solar cell efficiency tables (version 50)," *Progress in Photovoltaics: Research and Applications*, vol. 25, pp. 668-676, 2017.

[40] G.M. Kimball, P. Murcia, S. Chandra, and A. Bayman, "Methodology for improved cell integration based on distributed-element circuit analysis," in *42nd IEEE Photovoltaic Specialists Conference*, 2015, pp. 1-4. 10.1109/PVSC.2015.7355962.

[41] D.R. Hollars, R. Dorn, P.D. Paulson, J. Titus, and R.Z. Miasolé, "Large Area Cu(In,Ga)Se_2 Films and Devices on Flexible Substrates Made by Sputtering," *MRS Proceedings*, vol. 865, https://www.cambridge.org/core/article/large-area-cuingase2-films-and-devices-on-flexible-substrates-made-by-sputtering/94A2E4253D4719692F1B54DF937FA508, 2011.

[42] J. Kessler, J. Wennerberg, M. Bodegård, and L. Stolt, "Highly efficient Cu(In,Ga)Se_2 mini-modules," *Solar Energy Materials and Solar Cells*, vol. 75, pp. 35-46, 2003.

[43] I. Repins, S. Glynn, J. Duenow, T.J. Coutts, W.K. Metzger, and M.A. Contreras, "Required material properties for high-efficiency CIGS modules," in *Proc. SPIE*, 2009, p. 74090M.

[44] M.A. Green, K. Emery, Y. Hishikawa, W. Warta, and E.D. Dunlop, "Solar cell efficiency tables (version 46)," *Prog. Photovoltaics*, vol. 23, pp. 805-812, 2015.

[45] M.A. Green, K. Emery, Y. Hishikawa, W. Warta, and E.D. Dunlop, "Solar cell efficiency tables (Version 45)," *Progress in Photovoltaics: Research and Applications*, vol. 23, pp. 1-9, http://dx.doi.org/10.1002/pip.2573, 2015.

[46] H. Chen, F. Ye, W. Tang, J. He, M. Yin, Y. Wang, F. Xie, E. Bi, X. Yang, M. Gratzel, and L. Han, "A solvent- and vacuum-free route to large-area perovskite films for efficient solar modules," *nature*, vol. 550, pp. 92-95, http://dx.doi.org/10.1038/nature23877, 2017.

[47] M. Steiner, A. Bösch, A. Dilger, F. Dimroth, T. Dörsam, M. Muller, T. Hornung, G. Siefer, M. Wiesenfarth, and A.W. Bett, "FLATCON® CPV module with 36.7% efficiency equipped with four-junction solar cells," *Progress in Photovoltaics: Research and Applications*, vol. 23, pp. 1323-1329, 2015.

[48] S.R. Kurtz, D. Myers, and J.M. Olson "Projected performance of three-and four-junction devices using GaAs and GaInP," in *26th Photovoltaic Specialists Conference*, 1997, pp. 875-878.

[49] R. King, D. Law, K. Edmondson, C. Fetzer, G. Kinsey, H. Yoon, R. Sherif, and N. Karam, "40% efficient metamorphic GaInP/ GaInAs/ Ge multijunction solar cells," *Applied Physics Letters*, vol. 90, p. 183516, 2007.

[50] J. Geisz, S. Kurtz, M. Wanlass, J. Ward, A. Duda, D. Friedman, J. Olson, W. McMahon, T. Moriarty, and J. Kiehl, "High-efficiency GaInP/ GaAs/ InGaAs triple-junction solar cells grown inverted with a metamorphic bottom junction," *Applied Physics Letters*, vol. 91, pp. 023502, 2007.

[51] M. Wiemer, V. Sabnis, and H. Yuen "43.5% efficient lattice matched solar cells," in *Proc. SPIE*, 2011, pp. 810804-810805.

[52] F. Dimroth, M. Grave, P. Beutel, U. Fiedeler, C. Karcher, T.N. Tibbits, E. Oliva, G. Siefer, M. Schachtner, and A. Wekkeli, "Wafer bonded four-junction

Pursuant to the DOE Public Access Plan, this document represents the authors' peer-reviewed, accepted manuscript. The published version of the article is available from the relevant publisher.

GaInP/GaAs//GaInAsP/GaInAs concentrator solar cells with 44.7% efficiency," *Progress in Photovoltaics: Research and Applications*, vol. 22, pp. 277-282, 2014.

[53] A.C. Tamboli, J.F. Geisz, D.L. Young, M.A. Steiner, K.A. Horowitz, M.A. Woodhouse, M. Schnabel, T.W. Remo, S. Essig, and C. Allebe, "Raising the One-Sun Conversion Efficiency of III-V/Si Solar Cells to 32.8% for Two Junctions and 35.9% for Three Junctions," *Nature Energy*, vol. 2, 2017, article number 17144.

[54] J.D. McCambridge, M.A. Steiner, B.L. Unger, K.A. Emery, E.L. Christensen, M.W. Wanlass, A.L. Gray, L. Takacs, R. Buelow, and T.A. McCollum, "Compact spectrum splitting photovoltaic module with high efficiency," *Progress in Photovoltaics: Research and Applications*, vol. 19, pp. 352-360, 2011.

[55] M.A. Green, K. Emery, Y. Hishikawa, and W. Warta, "Solar cell efficiency tables (Version 32)," *Progress in Photovoltaics: Research and Applications*, vol. 16, pp. 435-440, http://dx.doi.org/10.1002/pip.842, 2008.

[56] D. Friedman, "Progress and challenges for next-generation high-efficiency multijunction solar cells," *Current Opinion in Solid State and Materials Science*, vol. 14, pp. 131-138, 2010.

[57] O.D. Miller, E. Yablonovitch, and S.R. Kurtz, "Strong internal and external luminescence as solar cells approach the Shockley–Queisser limit," *IEEE Journal of Photovoltaics*, vol. 2, pp. 303-311, 2012.

[58] E. Yablonovitch, O.D. Miller, and S. Kurtz, "The opto-electronic physics that broke the efficiency limit in solar cells," in *38th IEEE Photovoltaic Specialists Conference, 2012*, pp. 001556-001559.

[59] T. Takamoto, H. Washio, and H. Juso, "Application of InGaP/GaAs/InGaAs triple junction solar cells to space use and concentrator photovoltaic," in *40th IEEE Photovoltaic Specialist Conference, 2014*, pp. 0001-0005.

[60] G.S. Kinsey, W. Bagienski, A. Nayak, M. Liu, R. Gordon, and V. Garboushian, "Advancing efficiency and scale in CPV arrays," in *38th IEEE Photovoltaic Specialists Conference, Volume 2, 2012*, pp. 1-6.

Pursuant to the DOE Public Access Plan, this document represents the authors' peer-reviewed, accepted manuscript. The published version of the article is available from the relevant publisher.